ELSEVIER

Journal of Molecular Catalysis A: Chemical 155 (2000) 121–129

JOURNAL OF MOLECULAR CATALYSIS A: CHEMICAL

www.elsevier.com/locate/molcata

Intramolecularly selective decomposition of surfactant molecules on photocatalytic oxidative degradation over TiO_2 photocatalyst

Michitaka Ohtaki *, Hirofumi Sato, Hiroyuki Fujii, Koichi Eguchi

Department of Molecular and Material Sciences, Graduate School of Engineering Sciences, Kyushu University, 6-1 Kasugakouen, Kasuga, Fukuoka 816-8580, Japan

Abstract

Investigation on oxidative mineralization of various surfactants over TiO_2 photocatalyst reveals an anomalously retarded degradation of the trimethylammonium moiety in cationic surfactants. Model reactions using tetraalkylammonium chlorides as substrates confirm that the stepwise behavior of the mineralization time courses is ascribed to intramolecularly selective decomposition caused by a considerably slow degradation rate of the methyl groups directly bound to the quaternary nitrogen. A strong inhibition effect of bromide or iodide anions preventing the complete mineralization is also revealed.

Keywords: Semiconductor photocatalysis; Photoassisted mineralization; Photodegradation; Photodecomposition; Alkyltrimethylammonium surfactant

1. Introduction

Serious environmental concerns have arisen for water pollution caused by organic surfactants widely used for household and industrial purposes, because biodegradation of surfactants is generally very slow and sometimes ineffective [1–3]. Since depollution and bactericidal capabilities of TiO_2 semiconductor photocatalysts have been attracting keen interest and have begun to be commercialized in our daily lives [4], degradation of toxic surfactants through light-driven oxidation by semiconductor photocatalysis is expected to be promising as an inexpensive and environment-friendly alternative for water purification [5]. The strong oxidizing power of TiO_2 photocatalysts for degrading organic substances is mainly attributed to $\cdot OH$ and $\cdot OOH$ radicals formed from water (or OH^-) and dissolved oxygen, respectively, by the electron-hole pair generated by photoexcitation of valence electrons across the band gap of TiO_2 as shown in Fig. 1 [5,6].

Mineralization is conversion of carbon atoms in organic compounds into inorganic carbon species, which is usually CO_2. Photomineralization of organic substances by semiconductor photocatalysis has been investigated for a number of well-known and potential pollutants [5–8].

* Corresponding author. Tel.: +81-92-583-7465; fax: +81-92-573-0342; e-mail: ohtaki@mm.kyushu-u.ac.jp

1381-1169/00/$ - see front matter
PII: S1381-1169(99)00325-8

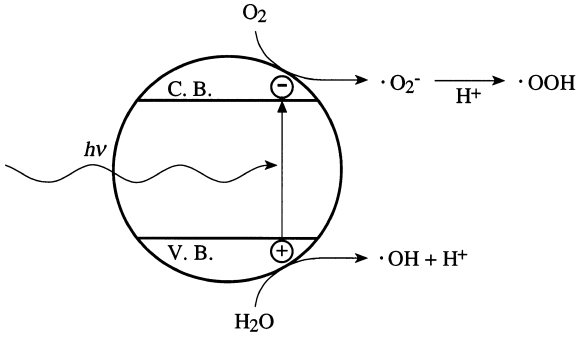

Fig. 1. Reaction mechanism of the formation of radicals as oxidizing agents on the illuminated TiO_2 photocatalyst.

Photocatalytic degradation of surfactants has also been studied over a wide variety of substrate molecules, and difference in the degradation rates between the surfactants with different polar head groups was observed at very low substrate concentrations [9–12]. However, there appears to be no report on apparent intramolecular selectivity reflecting differed reactivities between the component moieties of a surfactant molecule, which comprises two parts with highly contrasting nature; a hydrophobic long alkyl chain and a hydrophilic polar head group. Very recently, we have found that the photocatalytic oxidative mineralization of alkyltrimethylammonium chlorides shows an anomalous stepwise behavior, which suggests a consequence of different reactivities between the functional groups in a single surfactant molecule [13]. These observations deserve more detailed investigation for better understanding of the degradation mechanisms, which are still controversial. Moreover, information on the inhibiting factors in the photocatalytic treatment systems should be investigated in more detail, because in actual systems the photocatalytic purification of wastewaters will be carried out in the presence of a variety of contaminants. Here we report the investigation on the intramolecularly selective degradation behavior of alkyltrimethylammonium surfactants, and an inhibition effect of large halide counteranions; the latter was at first observed for the alkyltrimethylammonium system but was revealed to be a general phenomenon for light-driven mineralization of various surfactants over TiO_2 photocatalyst.

2. Experimental

Commercially obtained titania powder Nippon Aerosil P-25 was employed as the TiO_2 photocatalyst. The crystal phases comprising P-25 was determined as 70% anatase and 30% rutile from powder X-ray diffraction. The catalyst was pretreated at 400°C for 2 h in air beforehand. The following surfactants were used as the substrates: alkyltrimethylammonium chlorides and bromides (C_nTMA–Cl/Br, $n = 8$, 12, 16), and dodecylpyridinium chloride (C_{12}Py–Cl) are cationic, while sodium dodecylsulfate (C_{12}SO–Na), sodium dodecylphosphate (C_{12}PO–Na), sodium laurate (C_{11}CO–Na), sodium benzenesulfonate (BzSO–Na), and sodium dodecylbenzenesulfonate (C_{12}BzSO–Na) are anionic. Polyethyleneglycol monolaurate (C_{11}CO–PEG) was also examined as a nonionic surfactant. As model compounds for the trimethylammonium moiety of the C_nTMA–X surfactants, tetra(*n*-alkyl)ammonium chlorides (n-$C_nH_{2n+1})_4$N–Cl ($n = 1$, 2, 4, 5) were used as substrates. These reagents were of guaranteed grade and were used as received.

The photocatalytic reactions were carried out in a quartz reactor with a closed glass circulating system connected to a Shimadzu GC-8A gaschromatograph equipped with an Active Carbon packed column. The reaction mixture dispersing 0.25 g of P-25 in 100 ml of a 0.5 mM aqueous solution of the surfactant was irradiated with a 500-W xenon lamp through the flatten bottom of the reactor with continuous magnetic stirring under atmospheric air, with monitoring evolution of gaseous CO_2. The amount of CO_2 dissolved in the liquid phase was compensated by using Henry's law, the reliability of the calculation having been confirmed by releasing dissolved CO_2 into the gas phase by raising

temperature of the reaction mixture up to about 70°C.

The mineralization yield is defined as follows:

$$\text{Mineralization yield to } CO_2(\%) = \frac{\text{amount of } CO_2 \text{ evolved (mol)}}{\text{amount of total organic carbon in the substrate (mol)}} \times 100$$

A 100% mineralization yield to CO_2 stands for complete conversion of the organic carbon atoms in the substrate into CO_2.

3. Results and discussion

3.1. Stepwise behavior in complete mineralization of alkyltrimethylammonium surfactants

The photocatalytic mineralization time courses of various surfactants are shown in Fig. 2, with indications of the amounts of CO_2 to be evolved by the completion. Nearly the same behavior was observed for most of the substrates, for which CO_2 evolved linearly and reached straight ca. 100% mineralization. The CO_2 evolution rates were generally 70–80 μmol/h, showing no particular tendency over the substrates. For instance, C_{12}SO–Na, C_{12}PO-Na, and C_{11}CO–Na, those being anionic surfactants containing 12 carbon atoms per molecule but wearing different polar groups, showed virtually identical behavior. Moreover, BzSO–Na containing 6 carbon atoms needed a half the period of time for complete mineralization compared to the C_{12} species, and preferable degradation of the aromatic rings previously reported was thus undetected. Fig. 2 also compares cationic and anionic substrates fairly resembling in their molecular shapes, C_{12}BzSO–Na and C_{12}Py–Cl, clearly indicating no influence of the electrostatic charge of the polar groups. Furthermore, a nonionic surfactant, C_{11}CO–PEG, also gave the same CO_2 evolution rate. These results conclude that the behavior of photocatalytic mineralization over TiO_2 are essentially independent of the substrates under our experimental conditions, the degradation rate per carbon atom being identical regardless of the molecular structures. It has been well known that the Langmuir–Hinshelwood model holds for degradation of surfactants over TiO_2 photocatalyst. It has been accordingly confirmed that with increasing substrate concentration the rate limiting step becomes independent of the substrates [5]. The structure of the substrate

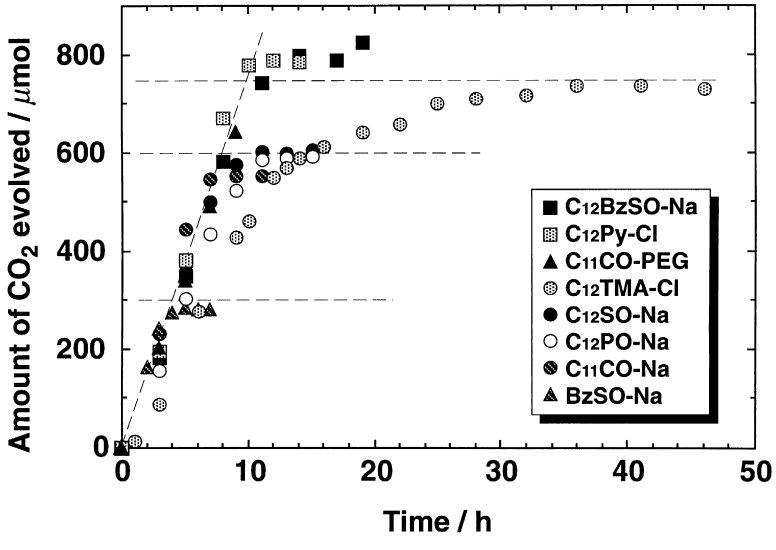

Fig. 2. Reaction time courses for photocatalytic oxidative degradation of various surfactants over P-25 TiO_2 photocatalyst.

molecules thereby slightly affects the reaction rate at moderate and high substrate concentrations, where the late limiting step is formation of radicals at the surface of TiO_2 [14]. Since the surfactant concentration is considered to be too excessive to the TiO_2 surfaces accessible for the substrates under our experimental conditions, the difference in the interactions between the surfactants and the TiO_2 surfaces, if any, would presumably give no effect on the degradation rate.

Nevertheless, alkyltrimethylammonium surfactants were found to exhibit anomalous mineralization behavior. Whereas the CO_2 evolution rate for C_{12}TMA–Cl at the initial stage was also almost the same (slightly smaller) as those for C_{12}PO–Na and C_{12}SO–Na having the same dodecyl chains, the evolution rate decreased to less than 0.2 times of the initial value after the CO_2 evolution reached ca. 600 μmol, and this reduced rate remained nearly constant until the complete mineralization. This behavior is depicted more clearly in Fig. 3, where the time course was redrawn in that of the mineralization yield with some other results already presented in Fig. 2. Note that, assuming the same degradation rate per carbon atom, the mineralization yield for the molecules containing lesser carbon atoms increases more rapidly because the mineralization yield corresponds to the fraction of converted carbon atoms in one molecule. The mineralization yield of 80%, where the degradation rate has dropped, corresponds exactly to the carbon fraction of the dodecyl chain (C_{12}/C_{15}) out of total carbon of the C_{12}TMA–Cl molecule. Moreover, the duration from the beginning until the CO_2 evolution rate changed is very the same as those needed for complete decomposition of C_{12}PO–Na and C_{12}SO–Na, for which the dodecyl chains account for the whole carbon atoms in the molecules. These facts strongly suggest that the abrupt decrease in the CO_2 evolution rate at the 80% mineralization yield observed for C_{12}TMA–Cl would have resulted from completion of preferential degradation of the dodecyl chain.

The probability of preferred degradation of the alkyl chains was further confirmed in Fig. 4 for photocatalytic mineralization of C_nTMA–Cl ($n = 8$, 12, 16). The time courses of the CO_2 evolution can be clearly divided into two regions for all the substrates. While the former

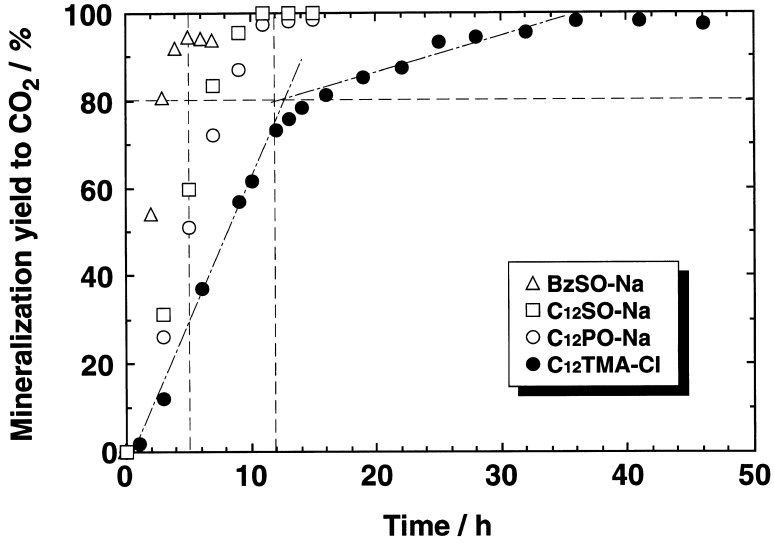

Fig. 3. Mineralization time courses for photocatalytic degradation of some anionic and cationic surfactants.

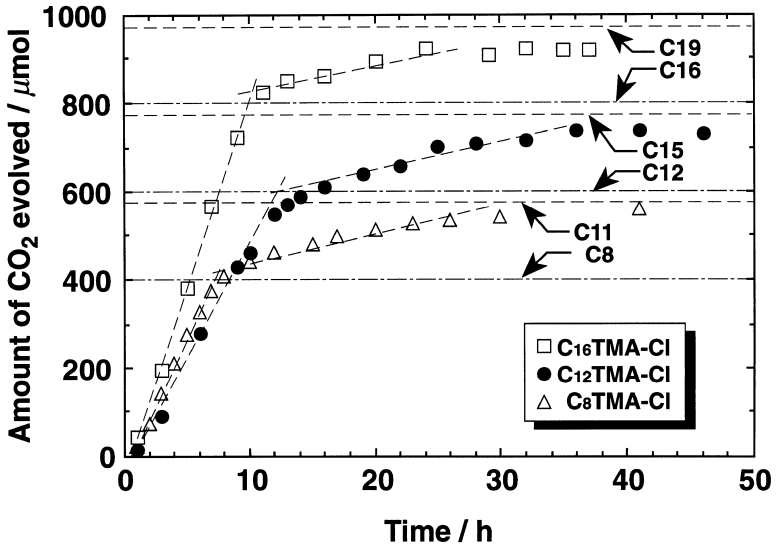

Fig. 4. Time courses of the CO_2 evolution on photocatalytic degradation of alkyltrimethylammonium surfactants.

region shows rapid degradation with the reaction rates slightly depending on the substrates, the latter region features slow CO_2 evolution yielding the virtually identical slope. The amounts of the evolved CO_2 when the degradation rate dropped were 400, 600, and 800 μmol, for C_8, C_{12}, and C_{16}TMA–Cl, respectively. Based on the amount of the substrates (50 μmol), these CO_2 amounts excellently agree with the molar number of the carbon atoms contained in their C_n alkyl chains. Beyond this 'bending' point, the slow evolution of CO_2 continued linearly up to the complete mineralization. The CO_2 evolution during the latter regions should therefore equal to the amount of the remaining carbon atoms (corresponding to three CH_3 groups of the trimethylammonium moiety) for all C_nTMA–Cl, and so the results were. It is hence plausible that the stepwise behavior observed on the photocatalytic mineralization of C_nTMA–Cl reflects a strong intramolecular selectivity which would lead to highly preferential degradation of the long alkyl chains. Since the reactions of the long alkyl chains and the trimethylammonium moiety should not be sequential but essentially competitive, it is implied that the aliphatic hydrocarbon chain decomposes much faster than the trimethylammonium moiety does. Consequently, after the mineralization of the carbon atoms in the long alkyl chains had almost been completed, degradation of the trimethylammonium moiety with relatively low reactivity would have been predominantly observed beyond the 'bending' point.

The results presented above suggest that, even similarly bound to the quaternary nitrogen atoms, the reactivity of the methyl groups could be much lower than the longer alkyl chains. We hence further carried out the photocatalytic mineralization of the tetraalkylammonium chlorides which have the four same alkyl chains as model compounds. Fig. 5 depicts the CO_2 evolution time courses for $(n\text{-}C_nH_{2n+1})_4N$–Cl ($n = 1$, 2, 4, 5), for those the methyl (Me), ethyl (Et), *n*-butyl (Bu), and *n*-pentyl (Pe) groups being quadruply attached to the quaternary nitrogen atoms, respectively. It is obvious that the mineralization completed straightforward for all four substrates. A slight disagreement of the final CO_2 amount observed for Et_4NCl may be due to some experimental errors because the reagent was strongly hygroscopic. The most outstanding feature of the results is a highly reduced degra-

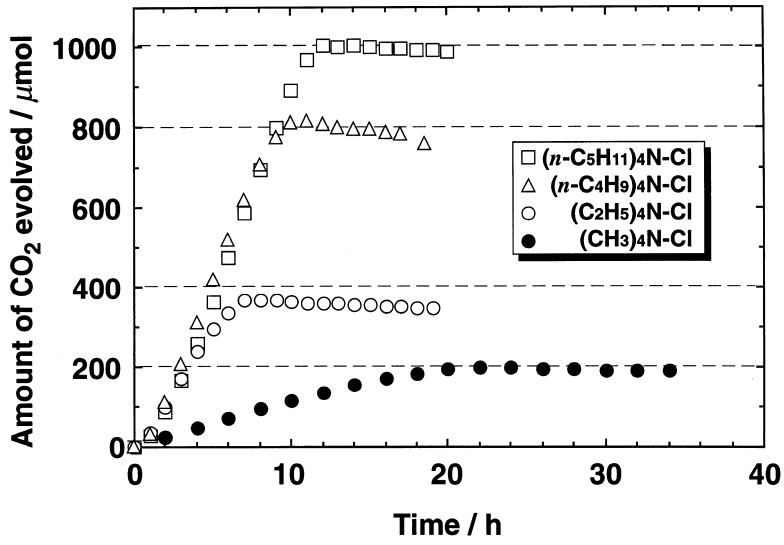

Fig. 5. Time courses of the CO_2 evolution on photocatalytic degradation of tetraalkylammonium chlorides.

dation rate observed only for Me_4NCl. The CO_2 evolution for Bu_4 and Pe_4NCl was rapid and completely linear until the completion. Even for Et_4NCl, only a small deviation from the same linear behavior was observed right before the completion; the slightly reduced evolution rate near the completion was still much higher than the initial rate for Me_4NCl. The excellent linearity of the CO_2 evolution observed for Et_4NCl and higher infers that, once the degradation of the alkyl chain initiated (probably from its terminal methyl group), the mineralization proceeds at the steady or sufficiently high rate until the last carbon atom will be converted. Although the mineralization of the intact methyl groups in Me_4NCl was revealed to be considerably slower than that of the longer alkyl groups, the linear CO_2 evolution until the completion for the ethyl and higher alkyl chains infers that an abrupt decrease in the decomposition rate on conversion of the last carbon atom directly attached to the quaternary nitrogen should be unlikely.

As an explanation of this anomalously low reactivity of the methyl groups of Me_4NCl, there seems to be at least two possible mechanisms; electrostatic repulsion between the cationic quaternary nitrogen atoms and the positively charged surfaces of TiO_2 [15], and a substantial change in the electron density on the (terminal) methyl carbon atoms caused by direct binding to the quaternary nitrogen. Since the initial step of oxidative degradation of organic compounds is considered to be hydrogen abstraction by the hydroxyl radicals [7,16], a decrease in the electron density on the carbon (and hence hydrogen) atom of the CH_3 group caused by a strong electron affinity of the quaternary nitrogen may tend to diminish the reactivity. However, a full rationalization of the low reactivity of the methyl group is still an open question at present.

3.2. Inhibition of complete mineralization caused by large halide counteranions

We have also revealed that halide counterions strongly influence the mineralization reaction of the C_nTMA–X surfactants [13]. In the preliminary experiments, we used C_8 and C_{16}TMA–Br in comparison with C_{12}TMA–Cl for investigation of the effect of the alkyl chain length, and found an incomplete mineralization of the substrates having Br^- counteranions. Fig. 6 presents the mineralization time courses of

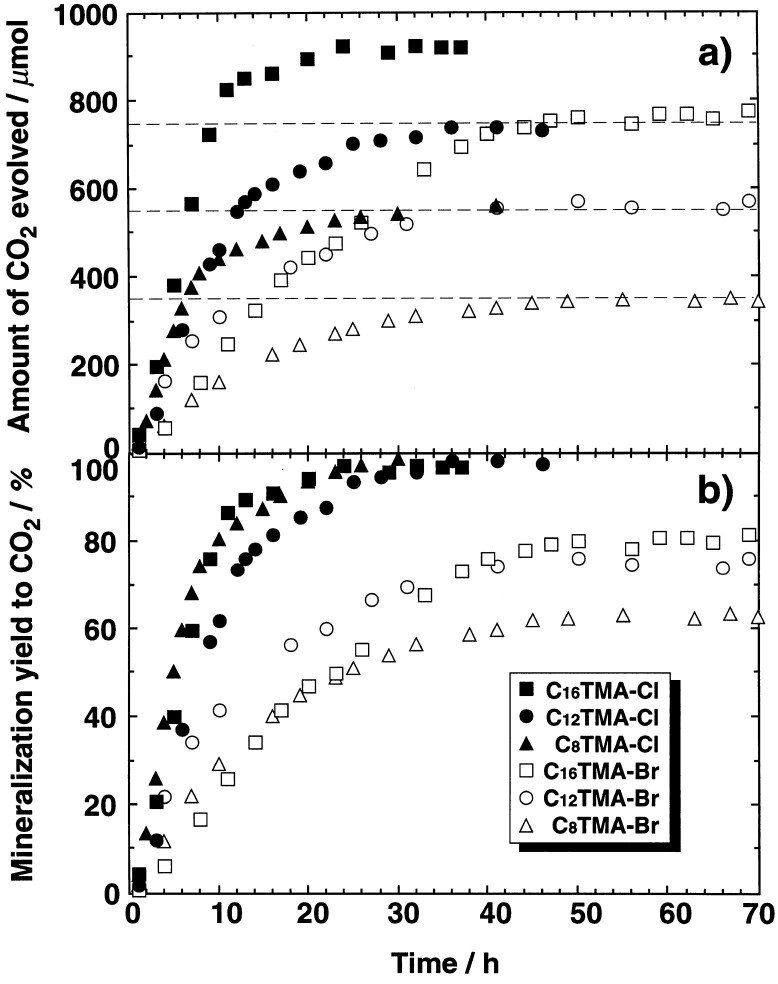

Fig. 6. Reaction time courses for photocatalytic degradation of alkyltrimethylammonium surfactants with Cl^- and Br^- counteranions; (a) the CO_2 evolution and (b) mineralization yield to CO_2.

C_nTMA–Cl and C_nTMA–Br ($n = 8$, 12, 16), showing the CO_2 evolution (a) and the mineralization yield (b). A complete mineralization having been attained for C_nTMA–Cl was obviously prevented for C_nTMA–Br, the final yields staying at around 60–80%. It would also be noteworthy that not only the final mineralization yields but the degradation rates were also markedly suppressed for the bromides. Interestingly enough, the final amounts of CO_2 evolution for the bromides coincide with those of the chlorides with the next shorter alkyl chains, i.e., the final CO_2 amount for $C_{16}(C_{12})$TMA–Br corresponds well to that for $C_{12}(C_8)$TMA–Cl. These results mean that the amount of CO_2 to be evolved but prevented by changing the counterion from Cl to Br equals to the difference in the carbon number between C_{16} (C_{12}) and C_{12} (C_8); four carbon atoms per molecule remained unconverted into CO_2 for bromides. This observation might be related to the fact that C_nTMA^+ ions have four carbon atoms directly bound to the quaternary nitrogen. However, we cannot be more assertive at present, because other surfactants were also found to undergo similar inhibition by Br^-.

Besides cationic C_nTMA–X, at least C_{12}Py–Cl (cationic) and C_{12}SO–Na (anionic) were re-

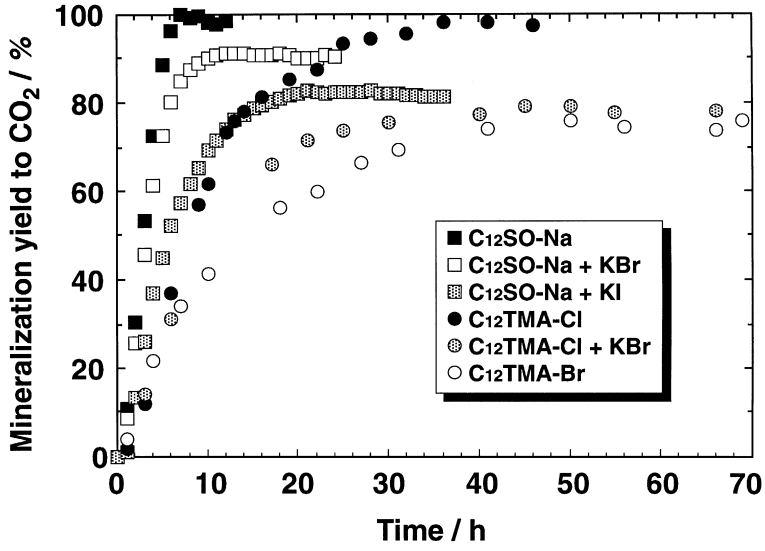

Fig. 7. Effects of coexisting halide anions on the mineralization time courses for photocatalytic degradation of sodium dodecylsulfate and dodecyl trimethylammonium surfactants.

vealed to undergo strong inhibition of complete mineralization in the presence of Br^-. Fig. 7 shows some representative data for C_{12}SO–Na and C_{12}TMA–X. As for C_{12}TMA–X, while the chloride attain complete mineralization as stated before, the final CO_2 evolution for the bromide was only 80% of completion. Moreover, addition of the equimolar amount of KBr to C_{12}TMA–Cl resulted in the very similar inhibition behavior, confirming that the coexistence of Br^- is responsible for the inhibition.

Not only cationic alkyltrimethylammonium surfactants, mineralization of anionic C_{12}SO–Na surfactant was also revealed to be inhibited by coexisting Br^-. Addition of the equimolar amount of KBr led to about the 90% mineralization yield at the end of the mineralization of C_{12}SO–Na. Furthermore, iodide anions were found to show the stronger inhibition ability, as seen in Fig. 7. It would be implied that the larger halide anions have the stronger inhibition ability for photocatalytic mineralization of various surfactants.

Although the mechanism of the inhibition effect of the heavier halide anions are not clear yet, supplemental addition of the substrate after the end of the incomplete mineralization in the presence of Br^- resulted in the identical (incomplete) mineralization time course, giving the same final mineralization yield after the second run. The excellent reproducibility of the incomplete mineralization time course thus clearly ruled out deactivation of the reaction site on the TiO_2 catalyst during the first run by such as surface adsorption of Br^-.

4. Conclusions

An anomalous stepwise behavior was observed on the photocatalytic oxidative degradation of the alkyltrimethylammonium surfactants over TiO_2 semiconductor photocatalyst. Investigation on the mineralization time courses and the model reactions using tetraalkylammonium compounds revealed that the stepwise behavior was a consequence of the considerably low reactivity of the methyl groups directly bound to the quaternary nitrogen; apparent intramolecularly selective decomposition thus emerged for alkyltrimethylammonium surfactants. Moreover, a strong inhibition effect of coexisting halide anions against the complete mineralization of

the surfactants was also discovered. Whereas the mechanism of the inhibition effect caused by the halide counteranions are not clear yet, the observed order of the inhibition strength was $I^- > Br^- \gg Cl^-$ (no inhibition); heavier halide anions appears to show stronger inhibition.

References

[1] R.D. Swisher, Surfactant Biodegradation, Marcel Dekker, New York, 1970.
[2] P. Gericke, R. Schmid, Tenside 10 (1973) 186.
[3] B.H. Fenger, M. Mandrup, G. Rohde, J.C.K. Sorensen, Water Res. 7 (1973) 1195.
[4] M.R. Hoffman, S.T. Martin, W. Choi, D.W. Bahnemann, Chem. Rev. 95 (1995) 69.
[5] D.F. Ollis, H. Al-Ekabi (Eds.), Photocatalytic Purification and Treatment of Water and Air, Elsevier, Amsterdam, 1993.
[6] A.L. Linsebigler, G. Lu, J.T. Yates Jr., Chem. Rev. 95 (1995) 735.
[7] O. Legrini, E. Oliveros, A.M. Braun, Chem. Rev. 93 (1993) 671.
[8] E. Pelizzetti, N. Serpone (Eds.), Homogeneous and Heterogeneous Photocatalysis (NATO Advanced Science Inst Series C: Mathematical and Physical Sciences, No 174), Reidel, Dordrecht, 1986.
[9] H. Hidaka, J. Zhao, E. Pelizzetti, N. Serpone, J. Phys. Chem. 96 (1992) 2226.
[10] H. Hidaka, K. Nohara, J. Zhao, K. Takashima, E. Pelizzetti, N. Serpone, New J. Chem. 18 (1994) 541.
[11] H. Hidaka, K. Nohara, J. Zhao, E. Pelizzetti, N. Serpone, J. Photochem. Photobiol. A: Chem. 91 (1995) 145.
[12] H. Hidaka, K. Nohara, J. Zhao, E. Pelizzeti, N. Serpone, C. Guillard, P. Pichat, J. Adv. Oxid. Technol. 1 (1996) 27.
[13] H. Fujii, H. Sato, M. Ohtaki, K. Eguchi, Chem. Lett. 1998 (1998) 251.
[14] C.S. Trurchi, D.F. Ollis, J. Catal. 122 (1990) 178.
[15] J. Zhao, H. Hidaka, A. Takamura, E. Pelizzetti, N. Serpone, Langmuir 9 (1993) 1646.
[16] Y. Mao, C. Schoneich, K.D. Asmus, J. Phys. Chem. 95 (1991) 80.